METABOLIC SYNDROME AND RELATED DISORDERS
Volume 19, Number 9, 2021

Pp. 491–497
DOI: 10.1089/met.2021.0055

Non-Alcoholic Steatohepatitis Severity Associates with FGF21 Level and Kidney Glucose Uptake

Souvik Sarkar, MD, PhD,[1,i] Shuai Chen, PhD,[2] Benjamin Spencer, PhD,[3] Xiaolu Situ, PhD,[4] Maryam Afkarian, MD, PhD,[5] Karen Matsukuma, MD,[6] Michael T. Corwin, MD,[3] and Guobao Wang, PhD[3]

Abstract

Background: Nonalcoholic steatohepatitis (NASH) is a severe form of fatty liver disease that has been shown to be associated with chronic kidney disease (CKD). Mechanism for the association of NASH with CKD remains unclear. In this study, we examined the association between NASH severity and kidney glucose uptake and the liver-secreted signaling molecule fibroblast growth factor 21 (FGF21).
Methods: Kinetic parameters for kidney glucose transport rate (K_1) and standardized uptake value (SUV) were determined using dynamic positron emission tomography after injection of ^{18}F-fluorodeoxyglucose. Liver biopsies were scored for NASH activity (inflammation and ballooning), fibrosis, and steatosis FGF21 was measured from fasting serum samples. Patients were categorized by liver biopsy and multivariate analyses were performed to evaluate the associations.
Results: Of 41 NASH patients 73% were females, 71% white, 51% with steatosis ≥2, 39% with NASH activity ≥4 and fibrosis ≥3. With severe NASH activity, kidney SUV significantly increased even when adjusted for underlying insulin-resistant (IR) state. Kidney K_1 decreased significantly in higher liver activity in unadjusted models but not when adjusted for IR. FGF21 decreased with severe liver activity in adjusted models ($P < 0.05$) and associated with kidney K1 but not SUV.
Conclusion: Our pilot data indicate that kidney glucose metabolism associates with NASH activity and FGF21 levels, suggesting a potential mechanism to NASH-induced CKD. Clinical Trials.gov ID: NCT02754037

Keywords: FDG, PET scan, kidney, NAFLD, fatty liver, multiorgan

Introduction

Nonalcoholic fatty liver disease (NAFLD) and its more severe form nonalcoholic steatohepatitis (NASH), is one of the most common liver diseases worldwide.[1] NASH is part of the multisystem disease metabolic syndrome. NASH itself is associated with kidney disease independent of underlying metabolic syndrome with its severity associated with worse kidney function.[2,3] However, there is a knowledge gap within the field regarding the relationship and mechanisms of extrahepatic disease in relation to NASH severity.[4] Closing this knowledge gap and characterization of extrahepatic disease with NASH severity is of clinical significance for development of therapies that may improve the liver disease but have unintended or beneficial consequences on other organs.

We propose a mechanism of altered glucose uptake and metabolism in extrahepatic tissues driven by hepatic steatosis, activity/inflammation, or fibrosis induced by NASH. Early steatosis from overnutrition can lead to decreased glucose uptake transporter expression,[5] whereas the inflammatory states such as NASH can be associated with increased glucose uptake transporter expression and uptake with activation of inflammatory pathways leading to tissue

[1]Division of Gastroenterology and Hepatology, Department of Internal Medicine, University of California, Davis, Sacramento, California, USA.
[2]Division of Biostatistics, Department of Public Health Sciences, University of California, Davis, Davis, California, USA.
[3]Department of Radiology, University of California, Davis, Sacramento, California, USA.
[4]Department of Statistics, University of California, Davis, Davis, California, USA.
[5]Division of Nephrology, Department of Internal Medicine, University of California, Davis, Sacramento, California, USA.
[6]Department of Pathology and Laboratory Medicine, University of California, Davis, Sacramento, California, USA.
[i]ORCID ID (https://orcid.org/0000-0002-9358-4257).

injury.[6–8] Altered glucose transport into the kidney cortical tissue may be anticipated due to increased apoptotic processes in renal tubular epithelial cells with the development of kidney disease such as in diabetic patients.[9,10] Positron emission tomography (PET) is a functional and molecular imaging modality with the widely accessible glucose analogue ^{18}F-fluorodeoxyglucose (FDG). FDG-PET is well known as an effective method for imaging glucose kinetics and metabolism related to glycolysis in cells.[11,12] Studies have shown the utility of static and dynamic FDG-PET imaging for studying physiological liver processes affected by obesity and NASH.[11,12] Static PET measures of glucose uptake such as standardized uptake value (SUV) have been shown to be correlative of renal tubular injury and function.[13,14] Previous studies have demonstrated the ability of dynamic FDG-PET parameters to measure biopsy-proven NASH activity.[15] Using glucose uptake as a surrogate measure for both insulin resistance and inflammatory changes that are central to NASH pathology, FDG-PET is well suited for multiorgan assessment of metabolic interactions.[12,16–19]

There is increasing evidence that the effect is modulated, in part, through secretion of ''hepatokines.''[20] These are proteins secreted primarily by hepatocytes and affect downstream metabolic processes, with fibroblast growth factor 21 (FGF21) being one of the primary hepatokines,[20] a positive metabolic regulator. Although FGF21 levels increase as a compensatory response in obesity and hepatic steatosis, a lack of FGF21 is associated with worsened metabolic disorders in NASH, leading to increase in inflammatory cytokines interleukin (IL)-6 and monocyte chemoattractant protein-1 (MCP-1).[21–23] It remains undetermined how NASH severity affects FGF21 levels and extrahepatic tissue glucose uptake. We hypothesize that NASH severity alters glucose metabolism through FGF21 as a precursor to future kidney disease. In this pilot study, we sought to characterize the association of NASH severity (defined by steatosis, activity, and fibrosis), kidney glucose uptake kinetics, and FGF21.

Materials and Methods

Study design and population

This was a single-center cross-sectional study, with enrollment of consecutive adult patients with NASH from 2016 to 2019. The study was approved by the University of California, Davis institutional review board and radiation use committee. Baseline clinical and laboratory values of all enrolled patients were recorded. Imaging studies were performed within 2 weeks to 6 months of liver biopsy (average time from biopsy to PET scan 8 ± 5 weeks).

Inclusion and exclusion criteria

Patients who had undergone liver biopsy for routine clinical care or for enrollment into other NASH clinical trials were approached for enrollment. Patients with biopsy-proven NASH, ≥18 years age, and able to provide informed consent were eligible to enroll. Patients who were pregnant, had a history of alcohol abuse, chronic hepatitis B or C, or other chronic liver disease, Hgb A1c >9.5% or inability to lie in the PET scanner for $\sim$1 hr were excluded from the study. The consent form and the study protocol were discussed in detail with the patients. Consented patients underwent the FDG-PET study as detailed hereunder and laboratory study for routine clinical parameters and hepatokines analysis.

Medical records review

The study coordinators and a hepatologist (S.S.) performed review of medical records to document patient demographics, laboratory values, medications, and presence of co-morbidities such as diabetes, hypertension, and hyperlipidemia.

Liver histology

Liver biopsies were scored according to the NASH-clinical research network (NASH-CRN) criteria[24] by a single expert pathologist. Steatosis was graded 0–3 based on percentage of hepatocytes containing fat droplets. NASH activity (range 0–5) was calculated as a sum of lobular inflammation (0–3), and ballooning degeneration (0–2). Liver fibrosis was assessed using the established NASH-CRN criteria.

PET scan and tracer kinetic modeling

Dynamic FDG-PET studies were performed with the GE Discovery 690 PET/computed tomography (CT) scanner. Diabetic patients were instructed to hold their dose of short acting insulin and/or long-acting insulin after midnight. Pre-PET blood glucose was measured for all patients. Patients were positioned to allow the liver to be contained within the axial field of view ($\sim$16 cm) of the PET/CT scanner. Each patient was injected with $\sim$10 mCi ^{18}F-FDG after a routine clinical protocol. Dynamic data acquisition was started immediately before the intravenous bolus administration and lasted for 60 min. Immediately before the PET scan, a low-dose CT scan was performed for attenuation correction of the PET images.

Tracer kinetic modeling. Region-of-interest (ROI) was placed on the right kidney cortex to extract regional time-activity curves (TACs). ROI placements were tuned and confirmed by an experienced abdominal radiologist. TACs were fitted using a two-tissue compartmental model with an optimization-derived dual-blood input function.[25] The FDG blood-to-tissue transport rate, denoted as K_1, was estimated from the TAC fitting. Glucose uptake was measured as the SUV at 1 hr post-FDG injection.

Hepatokine

FGF21, a liver secreted hepatokine, was measured from stored serum samples collected at the time of enrollment. The samples were assayed using Discovery assay at Eve Technologies (Calgary, Alberta, Canada).

Statistical analysis

All statistical analyses were done with SAS 9.4 (SAS Institute, Cary, NC). Statistical significance was assessed at the 0.05 level (two-sided). Patient characteristics were summarized using descriptive statistics. Spearman's correlation coefficients were used to evaluate the correlation between kidney kinetic parameters, liver disease scores

(steatosis, activity, and fibrosis, with four or five ordinal levels), and FGF21. This is a pilot/exploratory study. Initial sample size estimates suggested that an enrollment of 40 patients (assuming 60% high and 40% low inflammation) will have 80% power to detect a difference of 0.93 SD in log-transformed kidney SUV between the low- and high-inflammation stages. This is based on a two-sided two-sample *t*-test with significance level of 0.05.

Linear regressions were performed to evaluate the association between kidney kinetic parameters and liver disease stages (steatosis, activity, and fibrosis) and FGF21. Liver disease stages were recategorized into two or three levels in regressions. If the Spearman's correlation coefficient is significant (or near the edge), we performed unadjusted univariate analysis first. If the unadjusted analysis yields significant association, we further adjusted for patient characteristics [race, gender, age, body mass index (BMI), glomerular filtration rate (GFR), and homeostatic model assessment for insulin resistance (HOMA-IR)] in regressions to minimize potential confounding issues. Log-transformation was performed for K_1, SUV, and FGF21 to satisfy normality assumption, and hence fold changes (exponentiated coefficients) between the liver disease stages were reported.

Results

Patient characteristics

Forty-one biopsy-proven NAFLD/NASH patients were enrolled in the study and had reliable FDG-PET kinetic estimates of the kidney cortex. Baseline patient characteristics are shown in Table 1. In brief, 71% of the patients were non-Hispanic whites, 73% were female, average age 55 ± 11 years, mean BMI $34.4 \pm 5.7\,kg/m^2$, Hgb A1c $6\% \pm 0.8\%$ with 29% diabetics. Laboratory parameters show ALT 62 ± 50 mg/dL, creatinine 0.83 ± 0.15 mg/dL with mean GFR calculated by the chronic kidney disease (CKD)-EPI formula of 88.3 (range 56–127) mL/min/1.73 m^2, fasting insulin concentration 186.4 (range 0.8–1110.2) mIU/L, and HOMA-IR 8.9 (range 0.1–51.6) mg/dL. Pathology measures showed high steatosis (≥2) in 51%, activity (≥4) in 39% and fibrosis (≥3) in 39% of patients.

Table 1. Patient Characteristics

Characteristics	*All* n = *41*
Demographics	
Race/ethnicity	
Hispanic white	9 (22%)
Non-Hispanic white	29 (71%)
Other/unknown	3 (7%)
Female, *n* (%)	30 (73)
Age (years)	55 ± 11 (32–77)
BMI (kg/m^2)	34.4 ± 5.7 (24.4–47.4)
Past medical history	
Diabetes, *n* (%)	12 (29.3)
Hypertension, *n* (%)	20 (48.8)
Hyperlipidemia, *n* (%)	19 (46.3)
Laboratory	
ALT	62.1 ± 49.8 (10–217)
Creatinine	0.83 ± 0.15
GFR[a] (CKD-EPI)	88.3 ± 18.4 (56–127)
Insulin concentration	186.4 ± 256.0 (0.8–1110.2)
HOMA-IR	8.9 ± 11.6 (0.1–51.6)
Pathology	
Steatosis, *n* (%)	
<2	20 (49)
≥2	21 (51)
Activity[b]	
<4	25 (61)
≥4	16 (39)
Fibrosis	
<3	25 (61)
≥3	16 (39)

[a]CKD-EPI calculation of GFR.
[b]NASH activity (range 0–5) was calculated as a sum of lobular inflammation (0–3), and ballooning degeneration (0–2).
BMI, body mass index; CKD-EPI, Chronic Kidney Disease Epidemiology Collaboration; GFR, glomerular filtration rate; HOMA-IR, homeostatic model assessment for insulin resistance; NASH, nonalcoholic steatohepatitis.

Association of kidney glucose kinetics with liver histology

Kidney glucose uptake or SUV was positively correlated with NASH activity ($r = 0.31$, $P = 0.05$) (Fig. 1A), whereas kidney glucose transport rate or K_1 showed a negative correlation ($r = -0.36$, $P = 0.02$) (Fig. 1B). As shown in Table 2, in unadjusted analysis both kidney SUV and K_1 associated with severity of NASH activity determined by liver biopsy. There was significant (19%) increase in SUV in patients with severe NASH activity (grade ≥4) ($P = 0.02$). When adjusted for age, gender, BMI, or GFR, increase in SUV remained associated with NASH activity severity. Of note, the increase in SUV remained significant and independent of underlying insulin-resistant state determined by HOMA-IR (Model 4, Table 2) with overall increase by 28% with severe NASH activity. FDG transport rate K_1, in contrast, decreased by 31% (1–0.69) with high NASH activity (grade ≥3) ($P = 0.04$). The association was borderline significant ($P = 0.05$) when adjusted for age, gender, BMI, and GFR with K_1 decreasing 28% with high NASH activity. There was no significant association when further adjusted for HOMA-IR. Neither uptake nor transport rate associated with either histological liver steatosis or fibrosis severity.

Association of FGF21 with liver histology and kidney glucose kinetics

From the fasting FGF21 level measured in 29 patients there was a decrease of 44% in FGF21 level in patients with severe NASH activity in unadjusted analysis ($P = 0.04$) (Table 3). As FGF21 levels can be affected by BMI and insulin-resistant state, we adjusted for these in the multiple regression model. The inverse association with liver activity severity persisted with a 50% decrease in severe liver activity when adjusted for age, gender, BMI, and kidney function and 46% relative decrease when further adjusted for HOMA-IR ($P = 0.04$). FGF21 levels did not associate with liver steatosis or fibrosis severity.

We further analyzed whether the change in FGF21 associated with kidney glucose kinetics. FGF21 did not associate with kidney SUV. FGF21 associated significantly with glucose transport rate (K_1) in unadjusted analysis with a positive association noted between the two variables (Fig. 2). K_1 decreased by 16% (1–1/1.19) with decrease of FGF21 by 100 U ($P = 0.01$), with the association persisting

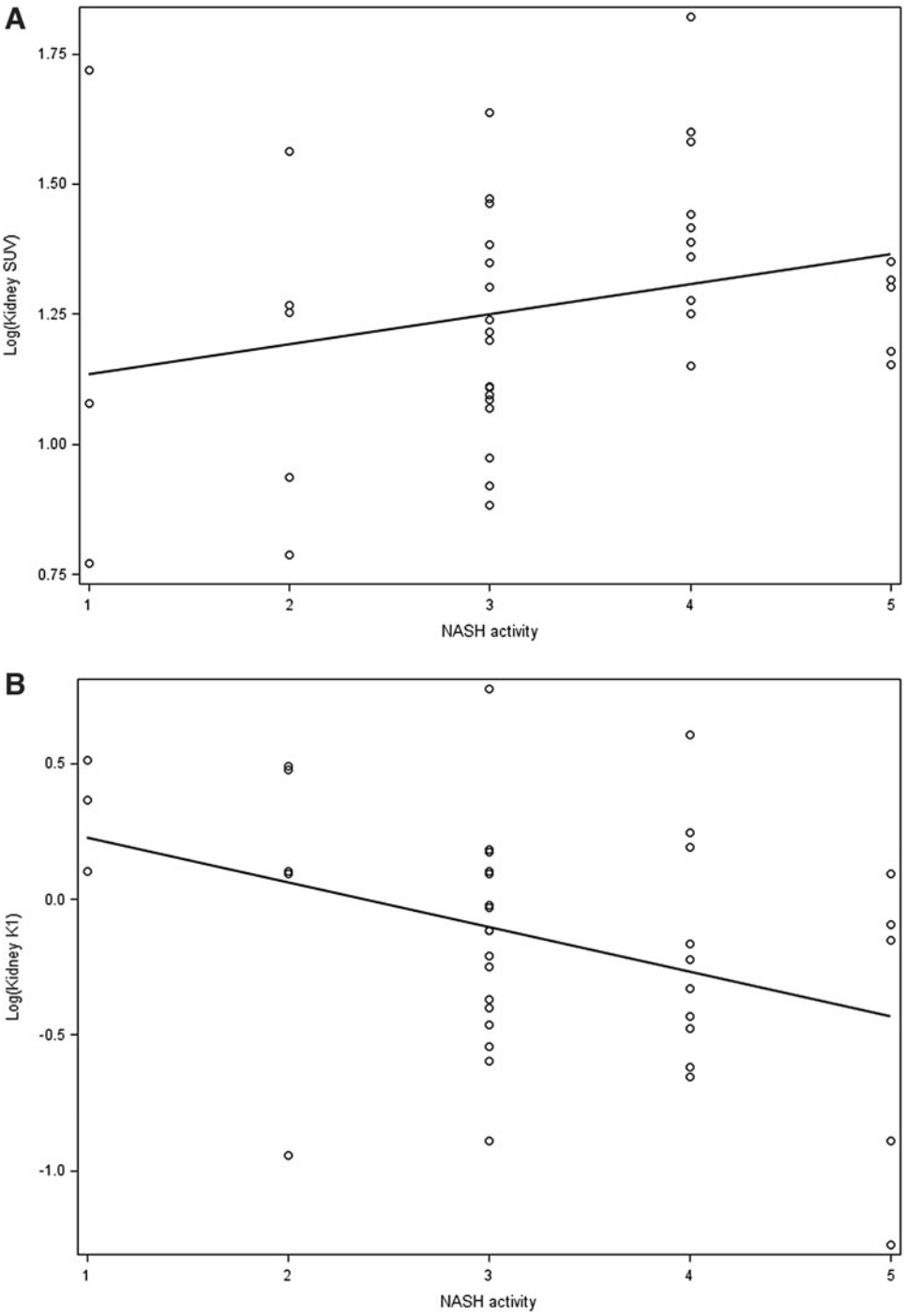

FIG. 1. Scatterplot of NASH activity and log [kidney **(A)** SUV, and **(B)** K_1) with regression line. NASH, nonalcoholic steatohepatitis; SUV, standardized uptake value.

even when adjusted for age, gender, BMI, kidney function, and HOMA-IR with a decrease in K_1 by 15% (1–1/1.18) with 100 U decrease in FGF21.

Discussion

CKD has been associated with NASH independent of other risk factors.[2] Progressive liver disease is presumed to affect downstream organs through altering insulin sensitivity that may alter glucose transport and metabolism.[2,20] Dynamic FDG PET enables determination of physiological processes in a human body. Prior studies using FDG PET by static scanning have identified the association of hepatic steatosis with increased hepatic glucose uptake and utilization, a phenomenon attributed to irreversible uptake by inflammatory cells and reversible hepatocyte uptake.[12] Our study utilizes dynamic FDG-PET scanning to determine the changes of glucose microkinetic parameters in the kidney with NASH severity defined by liver biopsy. Our data show that independent of age, gender, BMI, and more specifically of underlying insulin resistance (IR), kidney kinetic parameters associated with NASH activity.

Glucose uptake SUV is a semiquantitative parameter to quantify uptake using a simplistic method obtained from a single time point[26] and representative of the overall tissue metabolic process, including phosphorylation and glycolysis.

Table 2. Association Between Nonalcoholic Steatohepatitis Activity and Kidney Fluorodeoxyglucose Kinetics Based on Linear Regressions

	Model 1[a]		*Model 2*[b]		*Model 3*[c]		*Model 4*[d]	
Outcome	*Fold change (95% CI)*	P	*Fold change (95% CI)*	P	*Fold change (95% CI)*	P	*Fold change (95% CI)*	P
SUV (uptake)	1.19 (1.03–1.39)	**0.02**	1.17 (1.01–1.37)	**0.04**	1.20 (1.02–1.40)	**0.03**	1.28 (1.03–1.58)	**0.03**
K_1 (transport rate)	0.69 (0.49–0.98)	**0.04**	0.72 (0.52–1.01)	0.05	0.72 (0.51–1.00)	0.05	0.85 (0.54–1.34)	0.46

Values in bold denote $P < 0.05$.
For each outcome, the fold changes of outcome at high NASH activity with respect to low activity were reported.
SUV (overall glucose uptake); K_1 (glucose transport rate).
[a]Model 1 unadjusted.
[b]Model 2 adjusts for age, gender, and BMI.
[c]Model 3 adjusts for age, gender, BMI, and GFR.
[d]Model 4 adjusts for age, gender, BMI, GFR, and HOMA-IR.
CI, confidence interval; SUV, standardized uptake value.

Glucose transport rate K_1, in contrast, is a kinetic parameter determined from the TAC derived for 60 min of data. It represents the combination of blood flow and glucose transport from the vascular to the intracellular space. Increased glucose phosphorylation and activation of glycolytic pathways leads to development of oxidative by-products that are precursors to kidney damage and fibrosis.[27] Our data suggest that NASH-induced liver disease is intricately linked to the development of future kidney disease as noted by the decrease in the glucose transport rate but increase in overall uptake. Although the underlying insulin-resistant state present in many of these patients is the likely precursor to kidney pathology, liver disease itself strongly contributes to the process noted by its independent association with kidney SUV.

Furthermore, we found that FGF21 decreased with severe NASH activity. FGF21 has been associated with improved metabolic functions and insulin sensitivity.[20,28] Higher levels of FGF21 have been reported with increased NASH, believed to be a countermeasure to manage the metabolic stress.[28] FGF21 has been found to be a mediator in diabetic kidney disease. FGF21 deficiency aggravated diabetes-induced activity, oxidative stress, fibrotic effect, and chronic renal dysfunction.[29] Whereas introduction of FGF21 was noted to prevent the free-fatty acid-induced oxidative damage, apoptosis, and fibrotic effect.[29,30] We hypothesize that with severity of NASH, the compensatory mechanisms are disrupted leading to decrease in FGF21 and subsequent effect on oxidative processes and renal tubular epithelial cell apoptosis.[9,29] We do note a proportionate change in kidney glucose transport rate with FGF21 levels, suggesting a potential mechanistic pathway for the direct effect of liver pathology on kidney disease. It will be too simplistic although to associate only one factor to such a complex metabolic process and we anticipate multiple other pathways for this interorgan cross talk.

A few limitations are worth noting. The study is limited by the size of the cohort. The goal of this study was an exploratory analysis before undertaking a larger study. This study utilizes internal controls although future studies will include healthy controls. The axial size of the scanner of $\sim$16 cm limits the ability to perform dynamic FDG-PET scan of organs that are beyond the field of view. The EXPLORER total-body PET scanner is currently operational at our institution[31] and enables dynamic image capture of all organs simultaneously. This will allow elucidation of the effect of key metabolic tissues such adipose and muscle on the liver–kidney interaction. Finally, a caveat to consider is that although kidney SUV estimation is well established, dynamic kidney kinetic modeling still needs further development.

Conclusion

In conclusion, our study provides pilot data to define glucose FDG kinetics in the kidney in relation to liver disease in NASH patients. Our data show that kidney glucose transport and uptake/metabolism are altered with severity of liver activity. This effect is independent of other confounding risk factors and is, in part, associated with lack of liver-secreted molecules such as FGF21. It will be worth noting any beneficial effects of FGF21 therapeutic agents on NASH-induced CKD. Larger, diverse, and prospective

Table 3. Association Between Nonalcoholic Steatohepatitis Activity and Fibroblast Growth Factor 21 Based on Linear Regressions

	Model 1[a]		*Model 2*[b]		*Model 3*[c]		*Model 4*[d]	
Outcome	*Fold change (95% CI)*	P	*Fold change (95% CI)*	P	*Fold change (95% CI)*	P	*Fold change (95% CI)*	P
FGF21	0.56 (0.32–0.98)	**0.04**	0.48 (0.26–0.91)	**0.03**	0.50 (0.26–0.95)	**0.04**	0.54 (0.30–0.96)	**0.04**

Values in bold denote $P < 0.05$.
For each outcome, the fold changes of outcome at high NASH activity with respect to low activity were reported.
[a]Model 1 unadjusted.
[b]Model 2 adjusts for age, gender, and BMI.
[c]Model 3 adjusts for age, gender, BMI, and GFR.
[d]Model 4 adjusts for age, gender, BMI, GFR, and HOMA-IR.
FGF, fibroblast growth factor; FGF21, fibroblast growth factor 21.

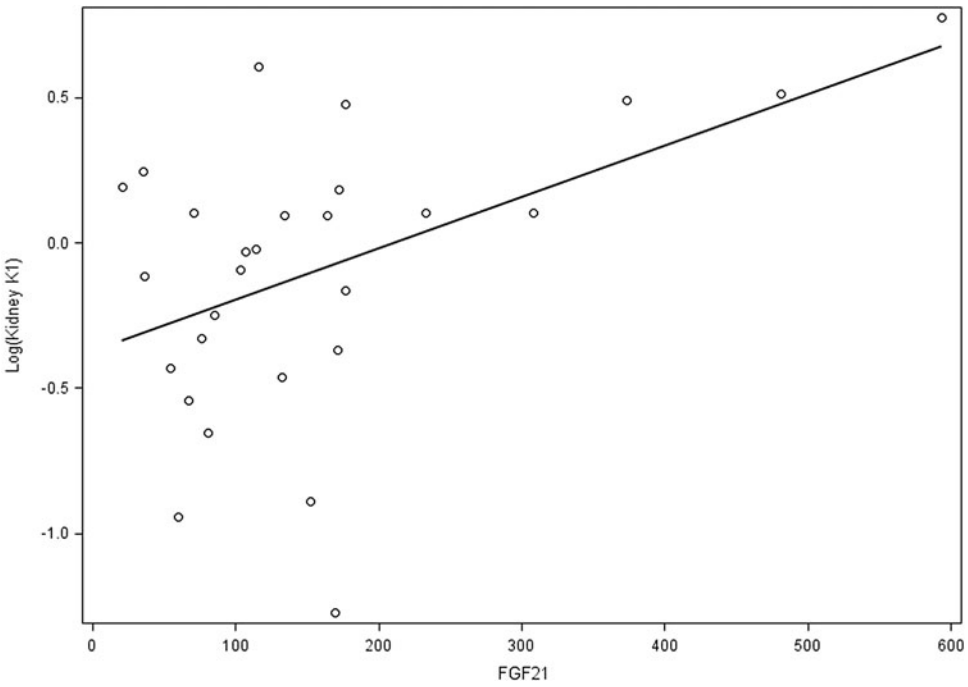

FIG. 2. Scatterplot of FGF21 and log (kidney K_1) with regression line. FGF21, fibroblast growth factor 21.

studies in NASH patients will be needed to understand the underlying physiology further and determine association of the PET and hepatokines data with established markers of kidney dysfunction.

Acknowledgments

We thank our patients for their participation in the study. We sincerely thank Joseph Zepeda and Chung-Heng Liu for their assistance in patient enrollment and study coordination, and Heather Hunt, Michael Rusnak, Mike Nguyen, and Denise Caudle for their assistances in PET/CT data acquisition.

Author Disclosure Statement

S.S. is in the advisory board for GENFIT, Eisai, 89Bio, LGChem, speaker for Eisai, grants (to UC Davis) from Gilead Sciences. No other authors have any relevant conflicts of interest.

Funding Information

University of California Davis start-up funds and UCD Collaborative for Diagnostic Innovation Grant to S.S. and G.W.

References

1. Chalasani N, Younossi Z, Lavine JE, et al. The diagnosis and management of nonalcoholic fatty liver disease: Practice guidance from the American Association for the Study of Liver Diseases. *Hepatology* 2018;67:328–357.
2. Byrne CD, Targher G. NAFLD as a driver of chronic kidney disease. *J Hepatol* 2020;72:785–801.
3. Musso G, Gambino R, Tabibian JH, et al. Association of non-alcoholic fatty liver disease with chronic kidney disease: A systematic review and meta-analysis. *PLoS Med* 2014;11:e1001680.
4. Adams LA, Anstee QM, Tilg H, et al. Non-alcoholic fatty liver disease and its relationship with cardiovascular disease and other extrahepatic diseases. *Gut* 2017;66:1138–1153.
5. Karim S, Liaskou E, Fear J, et al. Dysregulated hepatic expression of glucose transporters in chronic disease: Contribution of semicarbazide-sensitive amine oxidase to hepatic glucose uptake. *Am J Physiol Gastrointest Liver Physiol* 2014;307:G1180–G1190.
6. Peiro C, Romacho T, Azcutia V, et al. Inflammation, glucose, and vascular cell damage: The role of the pentose phosphate pathway. *Cardiovasc Diabetol* 2016;15:82.
7. Sokolovska J, Isajevs S, Rostoka E, et al. Changes in glucose transporter expression and nitric oxide production are associated with liver injury in diabetes. *Cell Biochem Funct* 2015;33:367–374.
8. Chadt A, Al-Hasani H. Glucose transporters in adipose tissue, liver, and skeletal muscle in metabolic health and disease. *Pflugers Arch* 2020;472:1273–1298.
9. Lv W, Booz GW, Fan F, et al. Oxidative stress and renal fibrosis: Recent insights for the development of novel therapeutic strategies. *Front Physiol* 2018;9:105.
10. Verzola D, Gandolfo MT, Ferrario F, et al. Apoptosis in the kidneys of patients with type II diabetic nephropathy. *Kidney Int* 2007;72:1262–1272.
11. Keiding S. Bringing physiology into PET of the liver. *J Nucl Med* 2012;53:425–433.
12. Keramida G, Hunter J, Peters AM. Hepatic glucose utilisation in hepatic steatosis and obesity. *Biosci Rep* 2016;36:e00402.
13. Pajenda S, Rasul S, Hacker M, et al. Dynamic 2-deoxy-2[18F] fluoro-D-glucose PET/MRI in human renal allotransplant patients undergoing acute kidney injury. *Sci Rep* 2020;10:8270.
14. Tian YG, Yue M, Nashun B, et al. The diagnostic value of [(18)F]-FDG-PET/CT in assessment of radiation renal injury in Tibet minipigs model. *J Transl Med* 2018;16:257.
15. Sarkar S, Corwin MT, Olson KA, et al. Pilot study to diagnose nonalcoholic steatohepatitis with dynamic (18)F-FDG PET. *AJR Am J Roentgenol* 2019;212:529–537.
16. Bural GG, Torigian DA, Burke A, et al. Quantitative assessment of the hepatic metabolic volume product in patients with diffuse hepatic steatosis and normal controls through use of FDG-PET and MR imaging: A novel concept. *Mol Imaging Biol* 2010;12:233–239.

17. Gastaldelli A, Gaggini M, Daniele G, et al. Exenatide improves both hepatic and adipose tissue insulin resistance: A dynamic positron emission tomography study. *Hepatology* 2016;64:2028–2037.
18. Iozzo P, Geisler F, Oikonen V, et al. Insulin stimulates liver glucose uptake in humans: An 18F-FDG PET Study. *J Nucl Med* 2003;44:682–689.
19. Liu G, Li Y, Hu P, et al. The combined effects of serum lipids, BMI, and fatty liver on 18F-FDG uptake in the liver in a large population from China: An 18F-FDG-PET/CT study. *Nucl Med Commun* 2015;36:709–716.
20. Meex RCR, Watt MJ. Hepatokines: Linking nonalcoholic fatty liver disease and insulin resistance. *Nat Rev Endocrinol* 2017;13:509–520.
21. Liu X, Zhang P, Martin RC, et al. Lack of fibroblast growth factor 21 accelerates metabolic liver injury characterized by steatohepatities in mice. *Am J Cancer Res* 2016;6:1011–1025.
22. Zheng Q, Martin RC, Shi X, et al. Lack of FGF21 promotes NASH-HCC transition via hepatocyte-TLR4-IL-17A signaling. *Theranostics* 2020;10:9923–9936.
23. Tanaka N, Takahashi S, Zhang Y, et al. Role of fibroblast growth factor 21 in the early stage of NASH induced by methionine- and choline-deficient diet. *Biochim Biophys Acta* 2015;1852:1242–1252.
24. Brunt EM, Kleiner DE, Wilson LA, et al. Network N.C.R., Nonalcoholic fatty liver disease (NAFLD) activity score and the histopathologic diagnosis in NAFLD: Distinct clinicopathologic meanings. *Hepatology* 2011;53:810–820.
25. Wang G, Corwin MT, Olson KA, et al. Dynamic PET of human liver inflammation: Impact of kinetic modeling with optimization-derived dual-blood input function. *Phys Med Biol* 2018;63:155004.
26. Mah KAC. Curtis, *PET-CT in Radiotherapy Treatment Planning,* 1st ed, Philadelphia, PA: Saunders; 2008.
27. Zhang G, Darshi M, Sharma K. The Warburg effect in diabetic kidney disease. *Semin Nephrol* 2018;38:111–120.
28. Barb D, Bril F, Kalavalapalli S, et al. Plasma fibroblast growth factor 21 is associated with severity of nonalcoholic steatohepatitis in patients with obesity and type 2 diabetes. *J Clin Endocrinol Metab* 2019;104:3327–3336.
29. Zhang C, Shao M, Yang H, et al. Attenuation of hyperlipidemia- and diabetes-induced early-stage apoptosis and late-stage renal dysfunction via administration of fibroblast growth factor-21 is associated with suppression of renal inflammation. *PLoS One* 2013;8:e82275.
30. Suassuna PGA, de Paula RB, Sanders-Pinheiro H, et al. Fibroblast growth factor 21 in chronic kidney disease. *J Nephrol* 2019;32:365–377.
31. Badawi RD, Shi H, Hu P, et al. First human imaging studies with the EXPLORER total-body PET scanner. *J Nucl Med* 2019;60:299–303.

Address correspondence to:
Souvik Sarkar, MD, PhD
Division of Gastroenterology and Hepatology
Department of Internal Medicine
University of California, Davis
4150 V Street; PSSB 3500
Sacramento, CA 95817
USA

E-mail: ssarkar@ucdavis.edu